J. Fluid Mech. (2007), *vol.* 591, *pp.* 21–42. © 2007 Cambridge University Press
doi:10.1017/S0022112007007598 Printed in the United Kingdom

Transient natural ventilation of a room with a distributed heat source

SHAUN D. FITZGERALD AND ANDREW W. WOODS

BP Institute for Multiphase flow, University of Cambridge, Cambridge, CB3 0EZ, UK

(Received 5 December 2006 and in revised form 4 June 2007)

We report on an experimental and theoretical study of the transient flows which develop as a naturally ventilated room adjusts from one temperature to another. We focus on a room heated from below by a uniform heat source, with both high- and low-level ventilation openings. Depending on the initial temperature of the room relative to (i) the final equilibrium temperature and (ii) the exterior temperature, three different modes of ventilation may develop. First, if the room temperature lies between the exterior and the equilibrium temperature, the interior remains well-mixed and gradually heats up to the equilibrium temperature. Secondly, if the room is initially warmer than the equilibrium temperature, then a thermal stratification develops in which the upper layer of originally hot air is displaced upwards by a lower layer of relatively cool inflowing air. At the interface, some mixing occurs owing to the effects of penetrative convection. Thirdly, if the room is initially cooler than the exterior, then on opening the vents, the original air is displaced downwards and a layer of ambient air deepens from above. As this lower layer drains, it is eventually heated to the ambient temperature, and is then able to mix into the overlying layer of external air, and the room becomes well-mixed. For each case, we present new laboratory experiments and compare these with some new quantitative models of the transient flows. We conclude by considering the implications of our work for natural ventilation of large auditoria.

1. Introduction

Natural ventilation can have a key role in the design of energy efficient buildings. Owing to concerns over comfort, there has been considerable effort to understand the fluid mechanics of natural ventilation in some detail. Many such studies have focused on steady-state natural ventilation flows and the associated temperature distribution (Linden, Lane-Serff & Smeed 1990; Linden & Cooper 1996; Cooper & Linden 1996; Linden 1999; Gladstone & Woods 2001; Caulfield & Woods 2002; Fitzgerald & Woods 2004). However, the transition to steady state can also be important, especially in buildings such as theatres, where the time scale of the transient flow may be comparable with the time of occupancy (Kaye & Hunt 2004; Linden 1999).

Previous studies of transient ventilation, reported in the literature, have considered either transient heating (Kaye & Hunt 2004) or transient draining (Linden *et al.* 1990) in isolation. It is the interaction between the draining flows associated with the initial difference in temperature between the interior and exterior and the upward displacement flows, associated with the heating, which we focus on herein. In order to remove the complexity of turbulent plume dynamics from the transient ventilation flow, we restrict attention to distributed sources of heating.

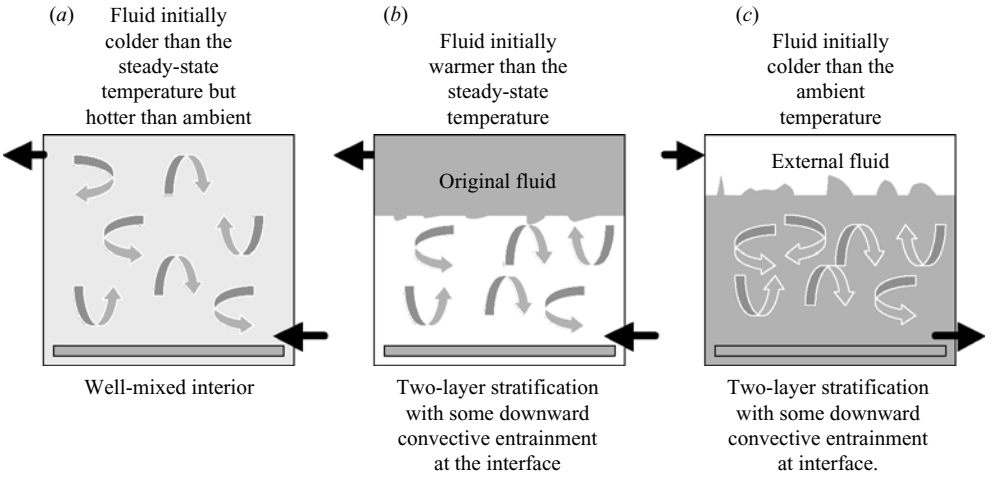

FIGURE 1. Schematic diagram of a room with heating at the base and vents at the top and bottom for ventilation. The three regimes correspond to (*a*) well-mixed upflow ventilation, (*b*) stratified upflow ventilation, and (*c*) stratified downflow ventilation.

Gladstone & Woods (2001) described the steady-state upward displacement ventilation which develops in this situation. However, the adjustment to this equilibrium may involve three different regimes, depending on the initial temperature of the space relative to both the final equilibrium temperature and the external temperature.

In § 2, we consider the transient ventilation when the initial room temperature lies between the exterior temperature and the equilibrium temperature of the room. In that case, the room remains well-mixed, while the temperature and ventilation rate gradually increase towards the new equilibrium (figure 1*a*). In § 3, we consider the case in which the initial temperature is hotter than the final equilibrium temperature. In this case, the inflowing air initially forms a layer which is colder than the original air within the room. As the flow proceeds, the temperature of the lower layer evolves towards the equilibrium temperature, while the original air vents from the room (figure 1*b*). We also show that, in this regime, the interfacial zone between the original and new fluid is subject to some mixing by penetrative convection from below (cf. Deardorff, Willis & Lilly 1969; Zilintekevich 1991). Finally, in § 4, we consider the case in which the room is initially colder than the exterior. In this case, the original fluid in the space initially drains from the lower vent, while a layer of external fluid accumulates above this layer (figure 1*c*). Again some penetrative convection develops at the interface, but eventually the lower layer attains the temperature of the upper layer and there is a larger scale overturn. The room then becomes well-mixed and adjusts to the final steady state through upflow displacement ventilation (§ 2).

2. Model of natural ventilation in a pre-heated room

We examine the transient ventilation in a room of vertical height H which is initially filled with air of constant temperature T_o with the exterior being of temperature T_e, where $T_e < T_o$. We assume that at time $t = 0$ a distributed heat source of strength Q per unit area is introduced at the base of the room, while vents of area A_t and A_b at the top and bottom of the room are opened (figure 1*a*). Following Linden (1999) and Gladstone & Woods (2001), we assume that the convection is of high Rayleigh

number and that, in the absence of strong density contrasts or gradients, it leads to a well-mixed space. If the heating rate is increased, the room temperature will also increase to a new equilibrium, while the room remains well-mixed during the transient evolution (figure 1*a*).

If the typical vertical dimension of the openings is small compared to the inter-opening distance, then the ventilation flow rate V is given by (Linden 1999)

$$V = A^{\star}[g\Delta T H/T_e]^{1/2} \tag{2.1}$$

where $T(z)$ is the temperature at height z in the room, $\Delta T = (1/H)\int_0^H (T(z) - T_e)\,\mathrm{d}z$, and $A^{\star}$ denotes the effective area of the vents,

$$A^{\star} = \frac{A_t A_b c_d}{\sqrt{0.5\left(A_t^2 + A_b^2\right)}}, \tag{2.2}$$

where c_d is the loss coefficient associated with the inertial flow through the vents (cf. Linden 1999; Gladstone & Woods 2001).

If we assume the building is very well insulated and has relatively small window area so as to minimize radiant heat losses, then to leading order, the heat supplied at the floor, QA, matches that associated with the ventilation together with the heating of the space:

$$AH\rho C_p \frac{\mathrm{d}\Delta T}{\mathrm{d}t} = QA - \Delta T \rho C_p V, \tag{2.3}$$

where A is the cross-sectional area of the room, ΔT is the difference in temperature between the room and the exterior, ρ is the density of air and C_p is the specific heat capacity of air. In steady state, the temperature difference between the interior and exterior air is related to the heat load according to the relation (Gladstone & Woods 2001)

$$\Delta T = \Delta T_s = \left[\frac{Q^2 A^2 T_e}{\rho^2 C_p^2 A^{*2} g H}\right]^{1/3}. \tag{2.4}$$

The well-mixed evolution towards the steady state occurs when the final steady temperature exceeds the initial temperature (figure 1*a*). In later sections we explore how the transient flow becomes stratified when the initial temperature is either greater than the final steady state, or colder than the exterior.

For convenience, in the remainder of our analysis we scale the temperature excess ΔT relative to ΔT_s, so that the dimensionless temperature difference relative to the exterior is given by $\theta = \Delta T/\Delta T_s$. We denote the initial value of θ by θ_o. We also scale time t relative to the time required to ventilate the room in steady-state conditions:

$$t_s = AH/V_s, \tag{2.5}$$

where V_s is the steady-state volume flux associated with the natural ventilation,

$$V_s = A^{\star}\,[g\Delta T_s H/T_e]^{1/2}, \tag{2.6}$$

so that the dimensionless time τ is given by $\tau = t/t_s$. This time scale is used as a reference in all the models in this paper.

The conservation of energy (equation (2.3)) may then be written in dimensionless form as

$$\frac{\mathrm{d}\theta}{\mathrm{d}\tau} = 1 - \theta^{3/2}. \tag{2.7}$$

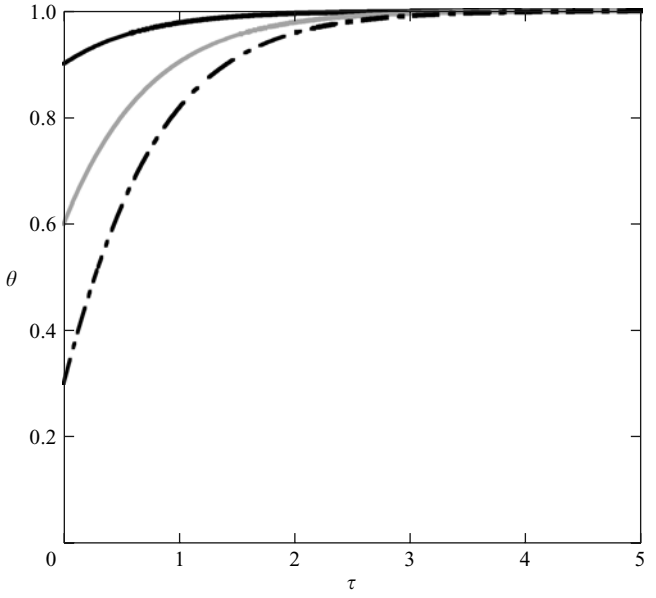

FIGURE 2. Evolution of the dimensionless temperature in the room θ as a function of time τ for the example cases of a room initially warmer than the exterior and cooler than the equilibrium temperature, in which $\theta_o = 0.9$, 0.6 and 0.3 as indicated by the solid black, solid grey and dashed black lines respectively.

The solution to (2.7) is given by the implicit relation

$$\tau = \mathscr{F}(\theta) - \mathscr{F}(\theta_o), \tag{2.8}$$

where

$$\mathscr{F}(\theta) = \frac{1}{3}\ln\left(\frac{\theta + \theta^{1/2} + 1}{\theta - 2\theta^{1/2} + 1}\right) - \frac{2}{3^{1/2}}\tan^{-1}\left(\frac{1}{3^{1/2}}\left(2\theta^{1/2} + 1\right)\right). \tag{2.9}$$

In figure 2 we illustrate the variation of temperature with time for three example cases in which $\theta_o = 0.9$, 0.6 and 0.3. This illustrates the nonlinear relation between the rate of heating and the initial temperature of the space, which in turn controls the initial ventilation flow rate.

3. Stratified case, $\theta_o > 1$

For the case in which the initial temperature is greater than the final steady temperature, $\theta_o > 1$, the upper layer of original hot air is displaced upwards by a lower, cooler layer of inflow. The new lower layer is initially cooler since the upward ventilation rate driven by the hot upper layer is faster than the steady-state ventilation rate, hence the heat supplied from the base of the cell is insufficient even to heat the lower layer to the steady-state temperature.

As the lower layer is heated up and deepens, it begins to convect and there may be some penetrative entrainment of the upper layer fluid into the lower layer (cf. Deardorff *et al.* 1969; Zilitinkevich 1991). Also, plumes of lower layer fluid may rise into the upper layer and produce an extended zone of intermediate temperature (figure 3). For high-Péclet-number convection, the effectiveness of such penetrative convection depends on the temperature contrast across the interface and

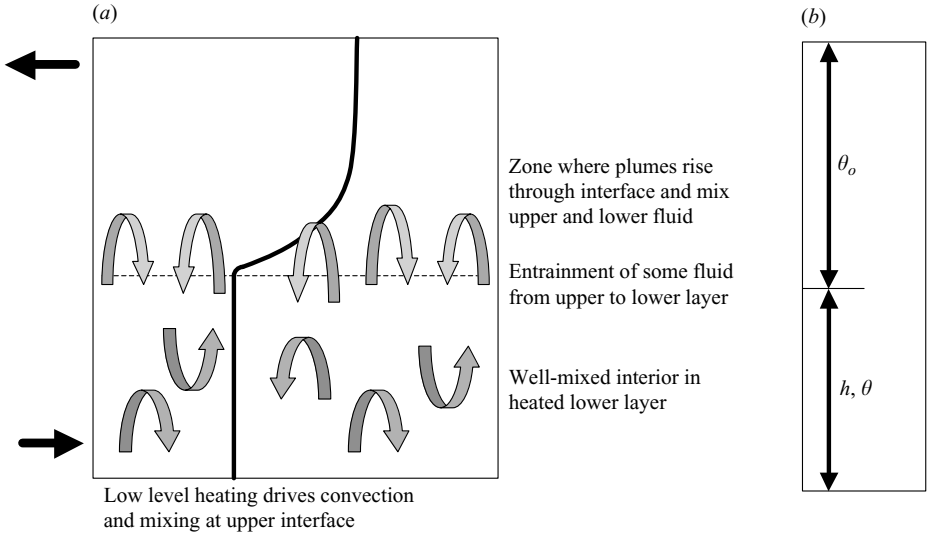

FIGURE 3. (*a*) Schematic of the process of mixing and penetrative convection at the interface between the lower heated layer and the hot upper layer, as observed in the experiments. (*b*) Illustration of the definition of the temperature and depth variables in the model.

the buoyancy flux driving the convection. The entrainment rate is sometimes modelled as being proportional to the inverse of the interfacial Richardson number or gradient Richardson number (cf. Zilintekevitch 1991). This is equivalent to assuming that the entrainment of upper layer fluid provides a buoyancy flux to the lower layer which is a fraction $k \sim 0.2 \pm 0.1$ of the buoyancy flux supplied by the heating at the base of the lower layer (cf. Zilintikevich 1991; Lister 1995). Although more complex parameterizations are possible, we adopt this simplified model here to illustrate the effect of any penetrative convection as the upper layer is ventilated from the room. Note that in § 5, we compare the predictions of this model to our new experimental data, and they show good agremeent with the model, to leading order. According to this model, we can write the rate of entrainment in the form

$$\rho C_p (T_u - T_l) \frac{\mathrm{d}h_i}{\mathrm{d}t} = kQ, \tag{3.1}$$

where T_u and T_l are the temperatures of the upper and lower layers, and h_i is the depth of the lower layer. The thickness of any mixed zone of elevated temperature near the interface may be estimated from the characteristic speed of the convective plumes and the distance to which they overshoot into the upper layer. In the Appendix we discuss the development of this mixed zone in more detail, arguing that in the building application, we expect that (3.1) should provide a leading-order description of the flow, unless the temperature contrast across the layers is small.

The evolution of the height of the interface h_i separating the lower and upper layers, and the temperature in the new lower layer of air, which we denote by θ, can be determined by considering conservation of mass and energy in the room (figure 3*b*). If we scale the interface height h_i relative to the height of the room H so that the dimensionless interface height is given by $h = h_i/H$ then, when $h < 1$, the ventilation flow through the room can be written as

$$\frac{V}{V_s} = q_o = \sqrt{\theta_o (1-h) + \theta h}, \tag{3.2}$$

where θ_o is the temperature of the upper layer. From the arguments above, we model the rate of entrainment across the interface by the relation

$$q_p = \frac{k}{\theta_o - \theta} \tag{3.3}$$

and so the rate of ascent of the interface is given by

$$\frac{\mathrm{d}h}{\mathrm{d}\tau} = \sqrt{\theta_o(1-h) + \theta h} + \frac{k}{\theta_o - \theta} \tag{3.4}$$

when $h < 1$. The conservation of energy in the lower layer can be expressed as

$$\frac{\mathrm{d}\theta h}{\mathrm{d}\tau} = 1 + \frac{k\theta_o}{\theta_o - \theta}. \tag{3.5}$$

Once the upper layer has been displaced from the room, and $h = 1$, then the model of § 2 describes the subsequent evolution of the room to steady state. We can assess the impact of the penetrative convection by comparing the predictions of the model for the cases $k = 0.2$ and $k = 0$. At early times, the above system of equations has asymptotic solution

$$h \sim \left(\theta_o^{1/2} + \frac{k}{\theta_o - \theta}\right)\tau \tag{3.6}$$

while the temperature of the lower layer

$$\theta \sim \frac{1+k}{\theta_o^{1/2}}. \tag{3.7}$$

We infer that in the limit $\theta_o \gg 1$, in which the initial fluid temperature far exceeds that of the steady state, the draining of the initially hot fluid is dominant, and the effects of heating are secondary as the upper layer vents. In the opposite limit, $\theta_o - 1 \sim 1$, in which the initial temperature is similar to but warmer than the final steady-state value, $\theta = 1$, the heating is also important. Note that in the limit $\theta_o - 1 \ll 1$, the temperature contrast between the layers becomes very small and the penetrative convection leads to a much deeper mixing zone. Indeed, as $\theta_o \to (1+k)^{2/3}$ the rate of penetrative convection, as predicted by the present model, becomes very large. Although this is a consequence of the simplified theoretical parameterization, it is a physical analogue of the limit in which the convective plumes in the lower layer approach the temperature of the upper layer fluid. In this limit, a more complete model of the mixing and stratification is required to describe the evolution of the system.

In figure 4 we show the time-dependent prediction of the evolution of the lower layer temperature (dashed thick line) and depth (solid thick line) for two example cases in which $\theta_o = 2.0$ and 10.0, and in which we set $k = 0.2$. For comparison, in this figure we also show thin dashed and solid lines which correspond to the model predictions in which penetrative convection is ignored ($k = 0$). In the case $\theta_o = 10$, during the initial period in which the original fluid is displaced out of the room, the rate of ascent of the interface, and hence volume flux, decreases with time. This is because the overall buoyancy driving the ventilation flow reduces. Since the flow rate decreases with time, but the heating rate is fixed, then the lower layer temperature increases progressively more rapidly, although starting with a relatively small value. Once the upper layer of initial fluid is completely displaced out of the room, the room becomes well-mixed and follows the flow regime of § 2. Note that the effects of penetrative convection are negligible in this case.

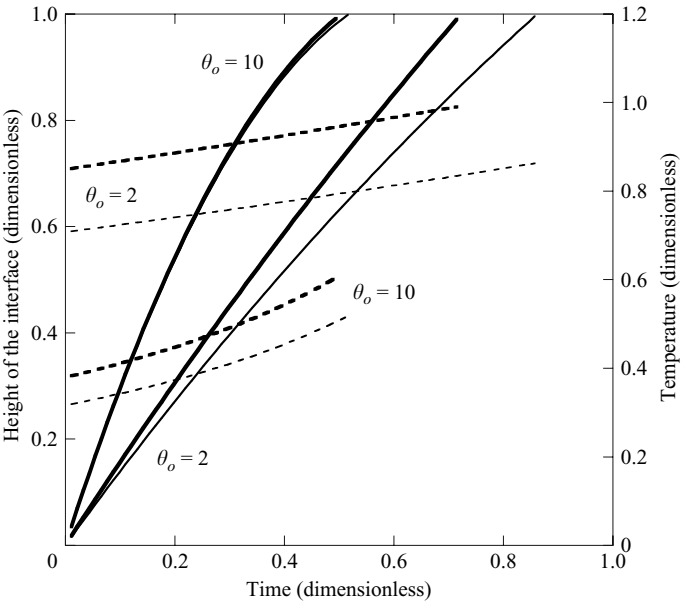

FIGURE 4. Prediction of the evolution of the dimensionless temperature of the lower layer θ (dashed lines) and interface height h (solid lines) as a function of time τ. Curves are given for two example cases corresponding to a room which is initially warmer than the exterior fluid with $\theta_o = 2.0$ and 10. For each case, two sets of lines are given; the thick lines correspond to the prediction of the model with $k = 0.2$ and the thin lines correspond to the prediction of the model with $k = 0$.

In the case $\theta_o = 2.0$, the initial rate of ventilation is much reduced so that the heating of the lower layer is more significant. This leads to a greater initial temperature of the lower layer. Also, comparing the model which includes the penetrative entrainment to the model which neglects penetrative entrainment (thick and thin lines), it is seen that the entrainment of the upper layer fluid into the lower layer leads to a warmer lower layer and faster ascent of the interface. As a result there is a more rapid convergence to steady state, although the increase in rate is relatively small (figure 5). The calculations imply that the two-layer model with no entrainment provides a reasonable bounding model if the initial temperature far exceeds the final steady-state temperature, so that the ventilation is dominant. However, as the temperature falls below the value $\theta_o = 2$, the effects of penetrative convection will become more significant, and the room becomes progressively more well-mixed; however, the two-layer model does provide a bound on the flow, and a guide to the rate of temperature increase in the lower layer following the onset of the ventilation.

Figure 5 illustrates how the time for the upper layer to vent from the room is influenced by the temperature of the upper layer and also by the effects of penetrative convection, according to the parameterization in our simplified model. The upper line illustrates the time to drain in the absence of penetrative convection, and shows how the time decreases with upper layer temperature, as expected. The lower line includes the prediction of the model accounting for the effect of the penetrative convection. It leads to similar predictions for large θ_o as the case in which penetrative convection is neglected. However, it also shows that for $\theta_o - 1 \leqslant 1$, the entrainment and mixing associated with the penetrative convection becomes important in mixing the layers, leading to rapid convergence to a well-mixed state.

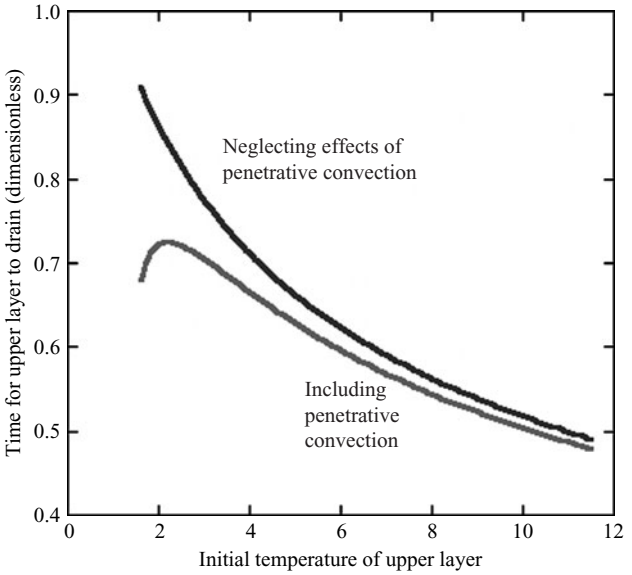

FIGURE 5. Dimensionless time for the interface to reach the ceiling for the case of a room initially warmer than the exterior as a function of the initial dimensionless temperature θ_o. The lower line includes the effects of penetrative convection ($k = 0.2$). The upper line corresponds to the prediction of the model in which we neglect penetrative convection ($k = 0$).

In the limit of a very hot initial temperature, $\theta_o \gg 1$, the interface reaches the ceiling at the approximate time $\tau \sim 2/\sqrt{\theta_o} \ll 1$. This corresponds to the time for the air initially in the room to drain in the absence of further heating (Linden *et al.* 1990).

4. Ventilation of a pre-cooled room, $\theta_o < 0$

If the room is initially colder than the exterior, $\theta_o < 0$, then the initial buoyancy within the room drives a downward flow. The external air entering from the upper vent is less dense than the air initially in place. It therefore ponds above the original air and a thermally stratified interior becomes established. As the downward ventilation continues, the lower layer is heated to temperature $\theta(t)$ by the distributed source of heat at the base of the system. This heating, combined with the decreasing depth of the layer, reduces the downward ventilation flow rate. Meanwhile, the convective plumes rising from the heat source at the base of the room, and through the lower layer of cold air are typically able to entrain some of the overlying layer of warm air, in a somewhat analogous fashion to the penetrative convection described in § 3. This reduces the rate of descent of the interface, even though fluid does vent from the base. Eventually, as the lower layer approaches the same temperature as the exterior, the air within the room becomes well-mixed. The continuing heating from the base then causes the fluid in the room to warm up relative to the exterior. Upflow displacement ventilation then develops until the temperature increases to the steady-state value. The balance between the ventilation, which causes the interface to descend, and the heating of the lower layer, which tends to reduce the ventilation rate, depends on the initial dimensionless temperature of the layer. If $|\theta_o| \ll 1$, then the draining flow is slow, and there is a short downflow transient during which the heating leads to the room approaching the temperature of the exterior; as this occurs, the penetrative

convection becomes very effective in mixing the lower and upper layers, and well-mixed upflow ventilation ensues. In order to model the transient downflow phase in this limit, a more detailed model of the penetrative convection and turbulent mixing is required since an extended zone of intermediate temperature will develop. However, for colder initial conditions, for which $|\theta_o| \geqslant O(1)$, the draining flow is relatively rapid, and a significant fraction of the lower layer can drain from the room before the lower layer is heated up to the temperature of the exterior, $|\theta| \sim 0$. In this case, we expect the mixing effects of the penetrative convection only to become significant just before the point at which the lower layer is heated to the temperature of the upper layer. In order to illustrate this, we follow the model of § 3 in which we account for the penetrative convection with the simple entrainment law (3.1).

The evolution of the lower layer is then given by conservation of heat and mass according to the following dimensionless relations. First, the volume flux through the room during the downflow phase, q_v, is driven by the negative buoyancy of the lower layer:

$$q_v = -\sqrt{h|\theta|}, \tag{4.1}$$

while the penetrative convection leads to deepening of this layer at a rate

$$q_p = \frac{k}{|\theta|}, \tag{4.2}$$

so that overall the lower layer depth evolves according to the relation

$$\frac{\mathrm{d}h}{\mathrm{d}\tau} = -\sqrt{h|\theta|} + \frac{k}{|\theta|}. \tag{4.3}$$

The conservation of energy in the lower layer has the form

$$\frac{\mathrm{d}\theta h}{\mathrm{d}\tau} = 1 - \theta\sqrt{h|\theta|}. \tag{4.4}$$

Combining these equations, and using the initial conditions, $\theta = \theta_o$ and $h = 1$ at $\tau = 0$, we find that at early time

$$|\theta| \sim |\theta_o| - \left(1 - |\theta_o|^{3/2}\right)\tau \tag{4.5}$$

and

$$h \sim 1 + \left(\frac{k}{\theta_o} - \sqrt{(|\theta_o|)}\right)\tau. \tag{4.6}$$

In figure 6 we show the evolution of the temperature in the lower layer, θ, as a function of time, for two cases in which the room is initially colder than the exterior, with $\theta_o = -2.0$ and -10.0. In each case, the temperature of the lower layer is predicted to increase progressively more rapidly with time as it drains through the lower vent. When the lower layer is initially cold, $\theta_o = -10$, the fluid nearly all drains from the base of the layer prior to the lower layer being heated and increasing to the temperature of the upper layer. At this stage there is a rapid overturn. In this case, the effects of penetrative convection are small, as may be seen by comparing the thin and thick lines. In the case in which $\theta_o = -2.0$, the draining flow is much slower. Eventually, as the temperature of the lower layer rises towards that of the upper layer, the penetrative convection becomes progressively more important, leading to mixing of some of the upper layer into the lower layer. The layer reaches a minimum depth and then begins to deepen as plumes rise high into the upper layer. Eventually its temperature rises to that of the exterior and the room becomes well-mixed. The

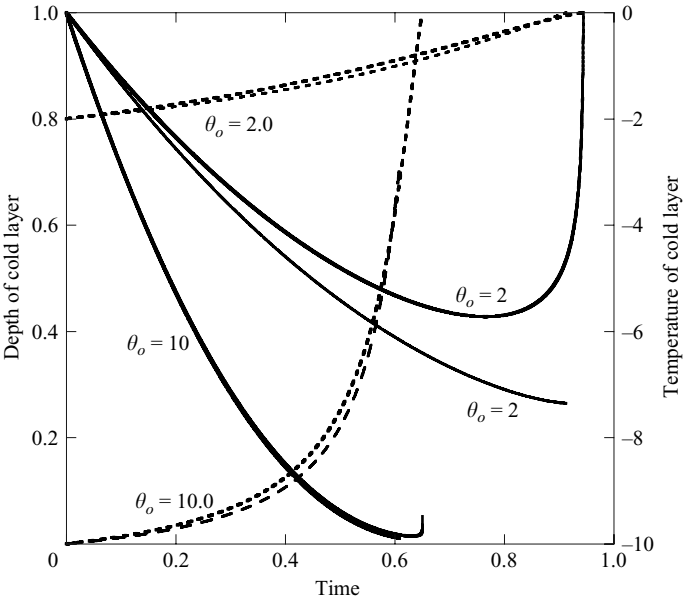

FIGURE 6. Evolution of the dimensionless temperature (dashed) and dimensionless depth (solid) of the lower layer θ as a function of time τ for the example cases of a room initially colder than the exterior in which $|\theta_o| = 2$ and 10 as shown. Thin curves correspond to the model prediction neglecting the effects of penetrative convection, while the thick lines include the simple parameterization of the penetrative convection.

details of the penetrative mixing in the final stages requires a more detailed model of the plume mixing process, and so the part of the curve showing a rapid deepening of the lower layer, just after a dimensionless time 0.9, should be viewed with caution. However, the present model does illustrate the impact of the penetrative convection prior to the point of overturn and mixing. Indeed, in figure 7 we compare the model predictions of the minimum depth of the upper layer as calculated in the cases in which there is no penetrative mixing (thin solid line) and using the simple model of penetrative mixing (thick solid line). This figure also shows the prediction of the time for mixing from both models, shown as thick and thin dashed lines. The calculations suggest that the penetrative convection leads to a smaller time for mixing when the initial temperature of the lower layer is only a small amount colder than the exterior, whereas the penetrative convection delays the overturn if the lower layer is much colder than the exterior.

In the limit $|\theta_o| \gg 1$, the turnover time approximates to the draining box time $\tau \sim 2/|\theta_o|^{1/2}$ (Linden *et al.* 1990). In the opposite limit, $|\theta_o| \to 0$, the initial room temperature is only slightly colder than the exterior so that once the heating commences, penetrative convection sets in and the room rapidly becomes well-mixed.

5. Experimental models

In order to test some aspects of the theoretical model predictions, we have conducted a series of analogue laboratory experiments using the water bath technique. In the experiments, a small Perspex tank is placed inside a large reservoir tank. The small tank is able to ventilate water to the large reservoir through high- and low-level

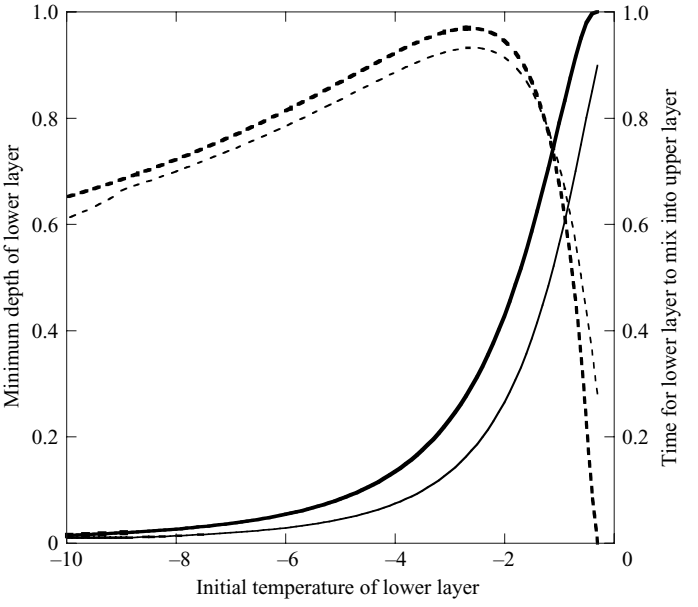

FIGURE 7. Variation with the initial temperature $|\theta_o|$ of (*a*) the minimum height of the interface h between the layers of cold and ambient fluid as a function of $|\theta_o|$, shown as the solid lines, and (*b*) the dimensionless time for the room to drain and become well-mixed, shown as dotted lines, for the case of a room initially colder than the exterior. Thick lines correspond to calculations including the model of the effects of penetrative convection ($k = 0.2$), while thin lines correspond to calculations neglecting the effects of penetrative convection ($k = 0$).

openings and it has a distributed heating source over the lower floor (cf. Gladstone & Woods 2001).

Using the scalings of § 3, then for typical operating conditions, with a distributed heat load on the floor of the tank of order 12.5 kW m^{-2}, we expect the convective speed of plumes in a layer of 20 cm depth to be about 0.4 cm s^{-1}. Also, given the applied heat flux, the convecting plumes have an excess temperature of order 0.7 °C relative to the lower layer. The Péclet number of such convection is about 850 in the heated lower layer, suggesting that there will be penetrative convection (Zilitinkevich 1991) with an erosion rate of about 0.06 cm s^{-1} across an interface with a 1 °C temperature contrast. The turbulent plumes may ascend a distance of order 1–2 cm above such an interface and this leads to an effective turbulent diffusivity of about 7×10^{-5} m^2 s^{-1}. In running the experiments in which a stratified temperature profile develops, and which persists for about 300–500 s, we therefore expect a diffusive mixed zone of several centimetres thickness to develop. This is smaller than the depth of the experimental system and so we expect that the leading-order models of §§ 2–4 provide a reasonable leading-order approximation to the flow regime.

5.1. *Method*

A small Perspex tank, 17.8 cm × 17.6 cm × 28.6 cm, was placed inside a large reservoir tank 48 cm × 88 cm × 43 cm, to model the exterior. A series of 16 ventilation holes, each of diameter 15 mm, were located in the roof of the tank, while a heating wire capable of delivering up to 500 W was positioned 1.0–1.2 cm from the base of the tank so as to provide a distributed heat source. The wire was arranged in a series of parallel sections, about 1 cm apart, across the whole floor of the tank in order to

produce a distributed heat flux. The base of the tank, below the wire, was open to allow fluid to enter in the upward displacement mode of natural ventilation, without the momentum of the inflow causing any mixing with the fluid in the tank. In the case of outflow through the base of the tank, the floor was initially sealed to the exterior but at the start of the experiment, a series of rubber stoppers were removed from the openings to allow the downward flow to commence. The heating wire was connected to a 30 V transformer via leads which were also connected to two digital multimeters, thereby enabling accurate measurements of applied current and voltage. Fourteen type-K thermocouples, accurate to $\pm 0.1\,^{\circ}\mathrm{C}$, were positioned at regular heights from the base of the small tank. The thermocouples were connected via two Pico Technology data loggers to a PC. A further thermocouple was placed within the reservoir tank to ensure that the temperature of the water below the top vents remained roughly constant. Temperatures were recorded every second throughout all experiments. The flow was observed using the shadowgraph technique, as well as through the use of tracer dyes.

Prior to commencing an experiment, the water in the reservoir and model tank was thoroughly mixed and the water was then allowed to settle. After roughly 15 minutes the tank was sealed with the rubber bungs and, for the experiments in which the interior temperature initially exceeds the exterior temperature, the heating wire and data loggers were switched on. Once the temperature within the tank had reached the desired level, typically several degrees centigrade greater than the external environment, the requisite number of rubber stops were removed from the roof of the Perspex tank to start the experiment. In the experiments in which the interior temperature was initially smaller than the exterior, before the experiment started the holes in the base of the tank were sealed below the heating wire. Then, to start the experiment, the bungs were removed from the base and the heating wire was turned on, so the system was allowed to drain, while being heated.

First we describe experiments in which we set $0 < \theta_o < 1$, in which case we expect the system to be well-mixed (§ 2). We then present some results for the case $\theta_o > 1$ for which a two-layer stratification develops with upflow ventilation (§ 3). Finally we turn to the case $\theta_o < 0$, when the interface descends into the tank, until eventually the lower layer heats up to the temperature of the exterior and the flow reverses to become upflow displacement ventilation (§ 4). In each case, we compare the experimental data with the predictions of the models.

5.2. *Results*

Well-mixed upflow ventilation: $0 < \theta_o < 1$

In the first experiment we report, the room was pre-heated to $1.5\,^{\circ}\mathrm{C}$ above the exterior. The interior fluid was dyed red and a heat flux of 280 W applied to the heating wire just before four vents were opened at the top and base of the experimental tank. This corresponds to the case $\theta_o = 0.42$. As expected from § 2, the data in figure 8(*a*) show that the room temperature remained approximately uniform with depth, suggesting that the room was well-mixed by the convection originating from the heated floor of the tank.

The photographs shown in figure 8(*b*) were taken 1 minute and 20 minutes after the vents were opened, and confirm that the dye was well-mixed throughout the room, becoming progressively more dilute with time. In figure 8(*c*) we compare the theoretical prediction for the evolution of the mean temperature in the room, as deduced from the model of § 2 (equation (2.7)), with the average of the temperature data recorded during the experiment. In the theoretical calculation, we assume the

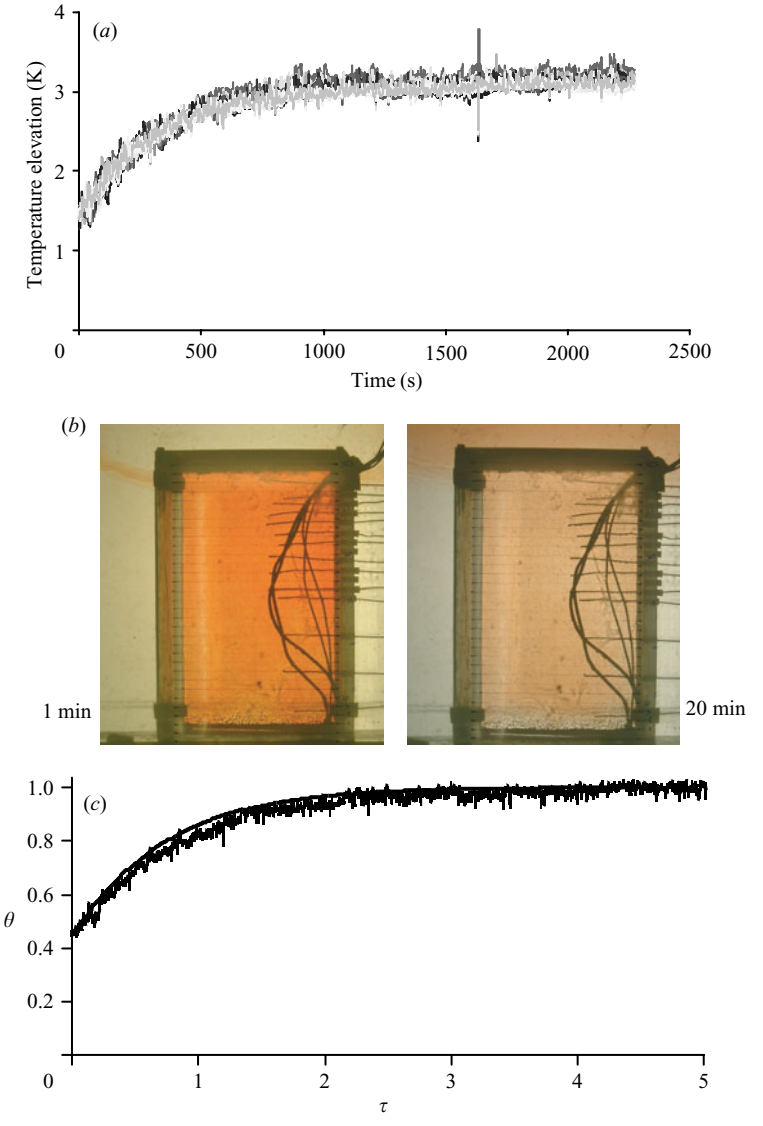

FIGURE 8. (*a*) Measured temperatures as a function of time in the tank heated by a distributed source and $\theta_o = 0.42$. Different symbols represent signals from each of the thermocouples. (*b*) Photographs taken 1 and 20 mins after commencement of ventilation showing that the room remained well-mixed throughout the duration of the experiment. (*c*) Dimensionless temperature of the interior derived from experimental data (thin noisy line) compared with the theoretical prediction (solid line).

thermal expansion coefficient of water is $3.3\times10^{-4}\,\mathrm{K}^{-1}$ (Haywood 1972). The transient evolution of the experiment agrees very well with the model prediction.

Room initially warmer than the final steady state: $\theta_o > 1$

In this case, we expect a two-layer stratification to develop. In the limit $\theta_o \gg 1$ the draining ventilation should be dominant but as θ_o decreases towards 1, the penetrative convection associated with the heating of the lower layer of the tank will become more important, leading to a more rapidly growing mixed zone between the two layers.

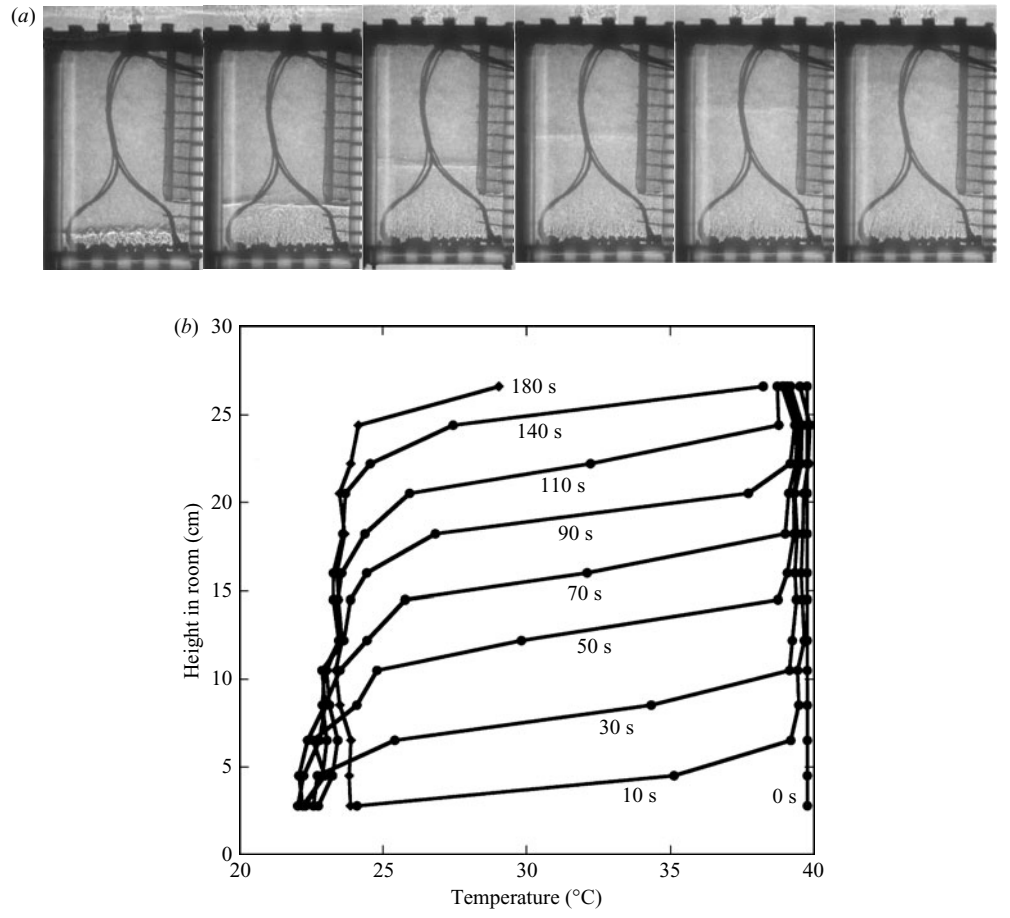

FIGURE 9. (*a*) Photographs taken at a series of times after commencement of the experiment in which $\theta_o = 5.25$, indicating that the upper layer of fluid originally in place is displaced vertically upwards during the transient evolution of the room, creating a two-layer stratification. (*b*) The vertical temperature profile in the experimental tank at a series of times, as shown on the figure, for the case in which $\theta_o = 5.25$. A clear thermal front is seen to rise through the room.

We carried out two experiments in which the fluid in the tank was initially heated up to 40 °C and then bungs were removed from either 2 or 4 vents on the roof of the tank to start the transient ventilation. In each case, the hot wire on the base of the tank supplied 480 W. In the case that 4 bungs were removed, the temperature at steady state would be 3.6 °C above the exterior, leading to an initial dimensionless temperature of $\theta_o = 5.25$ and with 2 bungs removed, the initial dimensionless temperature was $\theta_o = 3.34$.

Figure 9(*a*) presents a series of photographs of the experiment in the case $\theta_o = 5.25$. The photographs clearly show a well-defined front ascending through the tank, and this is corroborated by vertical profiles of temperature, taken at various times after the start of the experiment (figure 9*b*). The thermal profiles show a narrow transition zone of order 5 cm or less separating the cold lower layer from the warm upper layer. By analysing the data from the thermocouples, we determined the time at which the

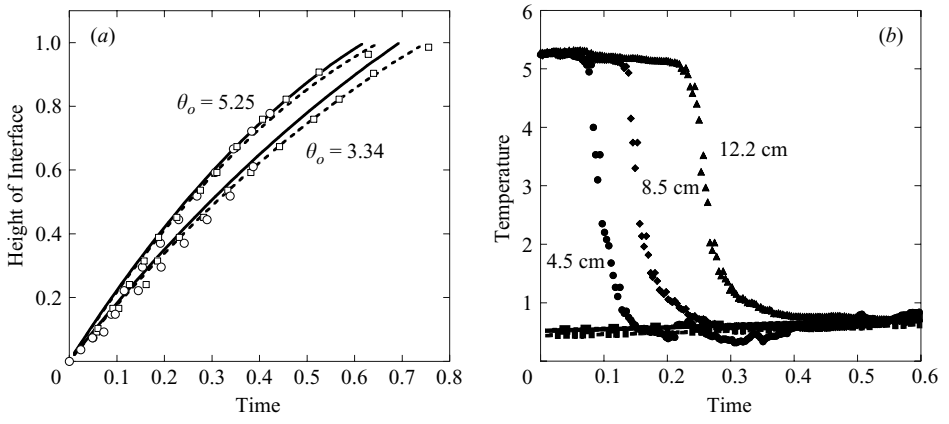

FIGURE 10. (*a*) Measured interface position as a function of time as deduced from the laboratory observations (circles) and the thermocouple data (squares). The data are compared with the theoretical prediction both accounting for penetrative entrainment, $k = 0.2$ (solid lines), and neglecting penetrative entrainment, $k = 0$ (dashed lines). Curves are given for the cases in which $\theta_o = 5.25$ and $\theta_o = 3.34$ as labelled. (*b*) Variation of the temperature as a function of time at dimensionless depths 0.16, 0.3 and 0.43 above the base of the tank for the experiment with $\theta_o = 5.25$. For comparison, curves are shown illustrating the temperature of the lower layer as predicted by the model in both the cases with penetrative entrainment (solid line) and neglecting penetrative entrainment (dashed line).

temperature of each thermocouple increased by 2 °C above the temperature of the lower layer, and hence at which the interface passed that thermocouple.

In figure 10(*a*) we present these data in the form of interface height as a function of time. In the same figure we have also plotted the height of the interface as a function of time as measured from the photographs shown in figure 9(*a*). There is a good correspondence between the two independent sets of data. For comparison, the predictions of the simple theoretical model, presented in § 3 (equations (3.4) and (3.5) are also shown in this figure. Two model curves are shown, the first accounts for penetrative convection using the parameter $k = 0.2$ while the second neglects the effects of penetrative convection ($k = 0$). Both models are in good agreement with the experimental data, but perhaps the model including penetrative convection is somewhat better. Similar results for the experiment with $\theta_o = 3.34$ are shown on the same plot, and again there is good agreement between the theory and the model.

In figure 10(*b*), we compare the predictions of the temperature of the lower layer as a function of time with the temperature recorded on three thermocouples, located at different heights above the base of the experimental tank. It is seen that once the interface rises past each thermocouple, the temperature of the thermocouple falls from the original high temperature of the upper layer to the colder temperature of the deepening lower layer. The data illustrate that there is a period during the passage of the interface when the temperature of the thermocouple fluctuates, and this is a result of the penetrative plumes mixing across the interface. Subsequently, as the interface and associated mixing zone rises higher in the tank, the temperature of the thermocouple stabilizes, but shows a gradual increase with time as the lower layer heats up to the final steady-state temperature. In figure 10(*b*), we also compare the prediction of the model of § 3 of the temperature of the lower layer in the tank (equations (3.4) and (3.5). Curves are given both for the model which includes the parameterized entrainment associated with penetrative entrainment ($k = 0.2$) and

for the model which neglects penetrative entrainment ($k = 0$). It is seen that the penetrative entrainment of warm upper fluid into the lower layer leads to a small increase in the temperature of the lower layer in accord with the observations.

We conducted a series of further experiments in which $\theta_o \leqslant 2$. In that case, plumes associated with the convection in the lower layer are able to penetrate much higher into the upper layer, thereby generating a much broader mixing zone, and the simplified theoretical picture of a two-layer system becomes less appropriate. Instead, the interior fluid develops a broader vertical temperature gradient as it drains from the upper opening, and converges to the new equilibrium. As mentioned in § 3 and 4, a more detailed model of this flow regime is required to model the mixing produced by the plumes as they rise higher above the interface.

Initial temperature smaller then exterior: $\theta_o < 0$.

As shown in § 4, if the room is initially colder than the exterior, then the fluid in the room drains from the base of the room while being heated up. If the interior is relatively cold compared to the final steady state, then the initial draining flow is rapid, and a two-layer thermal structure is expected to develop. The lower layer descends deep into the room prior to being heated towards the ambient temperature and mixing into the upper layer. To test the model, we carried out a series of experiments. In each experiment, relatively cold fluid was first placed in the tank, and then at the start of the experiment, the heater was turned on while a series of bungs were removed from openings in the top and base of the tank. We now present results from two experiments in which the fluid in the tank had initial temperature of 15.3 °C and 18.1 °C, while the external reservoir temperature was 24 °C. In the first experiment a heat load of 253 W was applied to the hot-wire system, which would lead to a steady upflow displacement ventilation temperature of 3.6 °C relative to the exterior, and hence a dimensionless initial temperature of −2.8, while in the second experiment a heat load of 333 W was applied, leading to a steady upflow displacement temperature of 4.2 °C, and hence a dimensionless initial temperature of −1.65.

In figure 11(*a*), we present a series of images of the experiment in which $\theta_o = -2.8$. These images illustrate how the fluid originally in the tank drains from the lower layer, with an initially sharp interface forming as warm external fluid enters from above. However, as the experiment procedes and the lower layer is heated up, the interface becomes progressively more convoluted and eventually a large-scale overturn occurs with the lower layer fluid mixing into the upper layer as the temperature of the lower layer reaches that of the exterior. Figure 11(*b*) illustrates how the vertical temperature profile in the tank evolves with time as this draining and heating procedes. A sharp temperature contrast develops as the warm external fluid replaces the cold fluid as it descends through the tank. The interface continues descending to just over half the depth of the tank, moving progressively more slowly as the lower layer warms up, until eventually the lower layer heats up to the temperature of the upper layer and the system becomes well-mixed. The thermocouple data illustrate that in the lower zone there is some fluctuation in temperature owing to convective plumes rising from the hot wire, but that the mixed zone near the interface remains less than 4–5 cm deep during the experiment.

We have analysed the thermal data in more detail for comparison with the model. First, in figure 12(*a*), we illustrate the variation of the temperature with time as recorded on two thermocouples located at dimensionless heights of 0.3 and 0.72 above the base of the tank. The descending interface rapidly passes the thermocouple in the upper part of the tank (at height 0.72), while the thermocouple lower in the tank

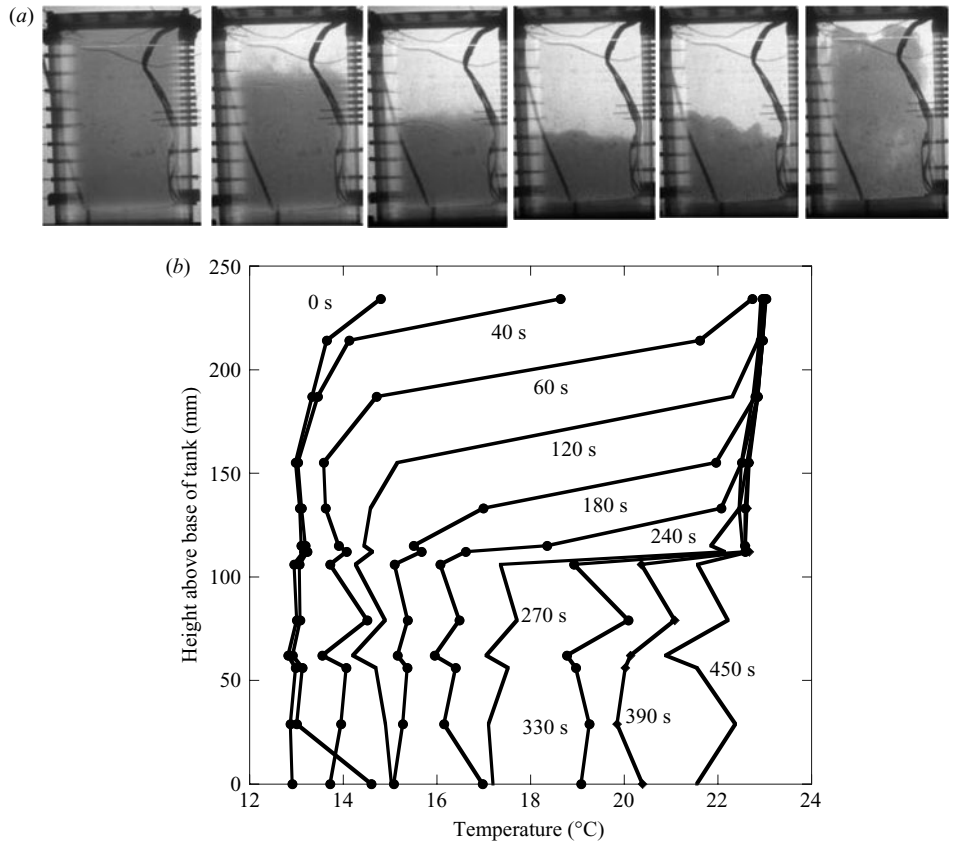

FIGURE 11. (*a*) Photographs taken at a series of times after commencement of the experiment in which $\theta_o = -2.8$, indicating that the fluid originally in place (shown darker) is displaced vertically downwards until heated to the temperature of the ambient at which point the system becomes well-mixed and upflow displacement ventilation continues. (*b*) Variation of the vertical temperature profile as a function of time in the tank for the case in which it was heated by a distributed source and $\theta_o = -2.8$. The times at which each temperature profile was recorded is shown on the curves.

(at height 0.3) remains below the interface. However, after a dimensionless time of order 0.6 the lower interface has descended close to but just above the thermocouple at 0.3. As the temperature of the lower layer rises above $\theta = -1$, convective plumes with increasing strength lead to progressively more fluctuation in temperature near the interface. As a result, the mixing zone deepens as the lower layer is heated towards the temperature of the upper layer and overturn ensues (cf. figure 11*a*). In this figure, we compare the predictions of the model of § 4 (equations (4.3) and (4.4), both accounting for the penetrative mixing ($k = 0.2$) and neglecting the mixing ($k = 0$). The model which accounts for the mixing of warm upper layer fluid into the lower layer provides a more accurate description of the evolution of the temperature of the lower layer. A similar evolution in the temperature occurs in the experiment in which $\theta_o = -1.6$, as may be seen in figure 12(*b*). One interesting observation in that data set is that the temperature fluctuations associated with the convective plumes primarily occur near the interface, and deeper in the lower layer the temperature remains more stable, although increasing with time. Again, the model accounting

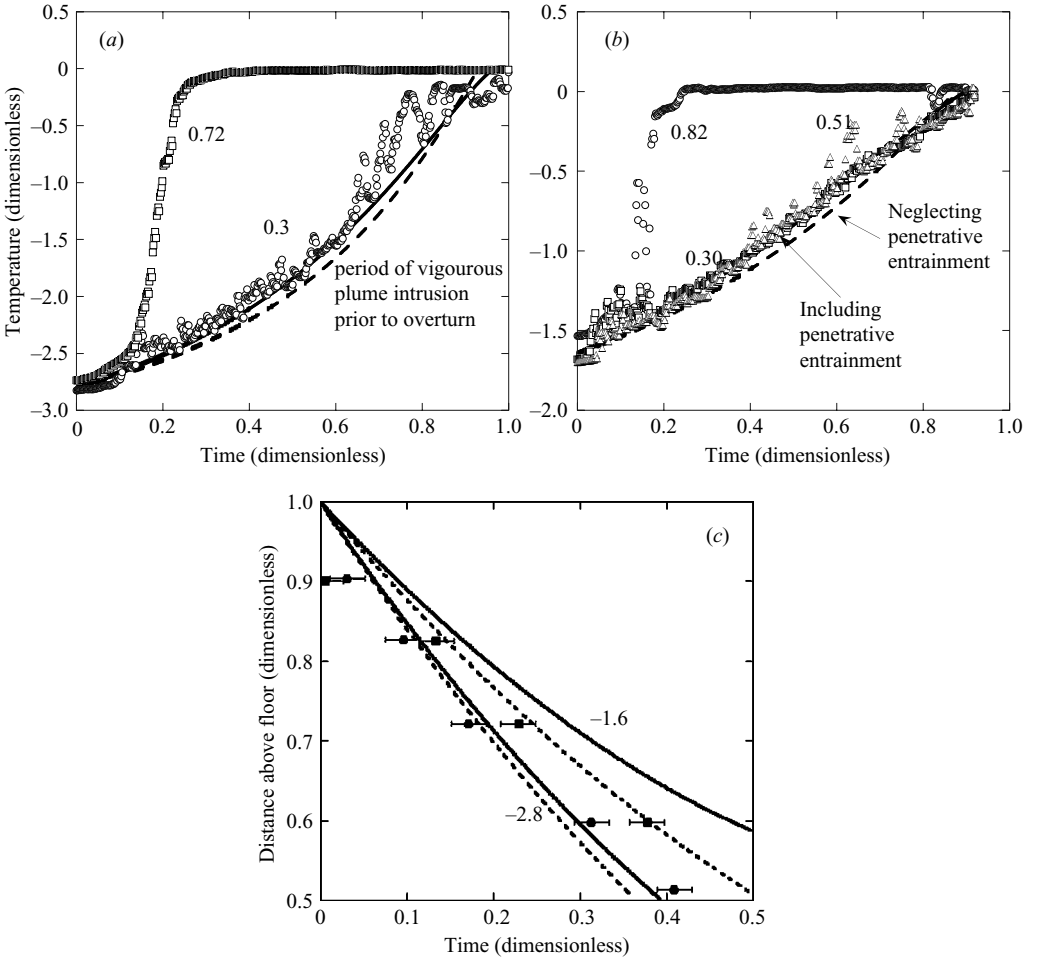

FIGURE 12. (a, b) Variation of the temperature as a function of time at several depths above the base of the tank for the experiments with (a) $\theta_o = -2.8$ and (b) $\theta_o = -1.6$. The dimensionless depth of each thermocouple is shown adjacent to the relevant data. For comparison, curves are shown illustrating the predictions of the model of the temperature of the lower layer, in both the cases with penetrative entrainment (solid line) and neglecting penetrative entrainment (dashed line). (c) Measured interface position (symbols) as a function of time as deduced from the thermocouple data, for the experiment with $\theta_o = -2.8$ and $\theta_o = -1.6$, as labelled on the graph. The data are compared with the theoretical prediction both accounting for penetrative entrainment (solid lines) and neglecting penetrative entrainment (dashed lines).

for penetrative entrainment provides a better match with the data. Finally, we have analysed the temperature data collected in both experiments to determine the time at which the temperature of each thermocouple increases by 1 °C above the temperature of the lower layer. Although there is some uncertainty in this time, owing to the temperature fluctuations associated with the convective plumes, we can use the data to estimate the time at which the interface passes each of the thermocouples in the upper part of the tank. In figure 12c, we show the height of the interface as a function of time. This is estimated from the thermocouples, by determining the height at which the temperature rapidly increases from that of the lower layer. We also show the predictions of the theoretical model presented in § 4, including both the cases

$k = 0.2$ and $k = 0$. Again there is reasonable agreement with the model. Inclusion of the penetrative entrainment predicts that the rate of descent of the interface is slower than for the the zero entrainment model, in accord with the data for the experiment with $\theta_o = -2.8$. We also note that although the zero entrainment model appears to fit our estimate of the experimental interface height for $\theta_o = -1.6$ better than the model including entrainment, these data only correspond to the early stages of the experiment; as the experiment progressed it became more difficult to estimate the interface height. However, for the main part of the experiment, prior to overturn, the temperature data (figure 12*b*) are in better agreement with the model which includes penetrative entrainment.

In a further experiment, we investigated the thermal evolution when $\theta_o = -1.1$. In this case, the role of penetrative convection becomes more substantial, with convective plumes mixing through the lower layer and leading to a much broader intermediate mixed zone. Again, as for the case $1 < \theta_o < 2$ (§ 5.2), a more complete model of the mixing associated with the large convective plumes rising through the interface is required to model the evolving temperature field in the case $-1 \leqslant \theta_o \leqslant 0$.

6. Conclusions and discussion

The results of the preceding sections illustrate that the transient evolution of a heated and ventilated room or other enclosed space depends on whether the room is initially hotter or colder than (i) the exterior and (ii) the final steady-state temperature of the room. If the room is warmer than the exterior, but colder than the steady-state temperature, then it remains well-mixed and gradually warms up, reaching the new steady temperature (§ 2). If the room is initially warmer than the final steady temperature, then upflow displacement ventilation develops, with a new cooler lower layer forming below the original fluid in the room. As the upper layer vents from the upper openings, the lower layer gradually heats up. In the case that the original and steady temperatures are relatively close, penetrative convection occurs across the interface, leading to some mixing of the upper layer fluid into the lower layer and a more gradual vertical temperature gradient develops. However, once the majority of the warm upper layer has vented from the room, the room becomes well-mixed and then gradually adjusts to the steady temperature. If the room is colder than the exterior, then initially air drains downwards through the room, with external air forming a deepening relatively warm upper layer (§ 4). As the lower layer is heated and drains, the rate of descent of the interface decreases, and some penetrative convection again develops at the interface, leading to some mixing of upper layer fluid into the lower layer. This mixing becomes more important as the magnitude of the temperature of the lower layer relative to the exterior decreases. Eventually, the lower layer reaches a minimum depth, and as it continues to heat up towards the exterior temperature, it becomes mixed into the upper fluid, leading to a well-mixed interior. As the heating continues, upflow ventilation then develops, and the room heats up to the final steady state.

For each regime we have developed a simple mathematical model to predict the evolution of the system with time. In the cases in which two-layer stratification develops, the model accounts for the effect of the penetrative entrainment across the two layers in the case that the ventilation flow is dominant, and the penetrative convection weak. In those cases our simplified models provide a reasonably good leading-order description of the evolution of the temperature and stratification in the space, and we have successfully tested the model predictions with new laboratory

experiments. However, if the initial temperature is hotter than but close to the final steady-state temperature, or close to but colder than the exterior temperature, then the penetrative convection is more significant and a more complete model for the development of a zone of intermediate temperature is required. This awaits a more complete model of the turbulent heat exchange across such interfaces.

It is of interest to apply the results to the ventilation flows which may develop in an auditorium. For example, we consider an auditorium with area 2000 m^2 and vertical extent 20 m and an audience of 500 people. Such a space will have a heat load of order 70 kW including both the people and lighting loads. Using the results of § 2, we infer that with a vent area of $A^\star = 1.26$ m^2, a steady-state displacement ventilation flow would develop with a temperature elevation of 15 °C relative to the exterior. Also, from § 2, it follows that the time scale associated with the establishment of this flow would be of order 5000 s or 1.3 hours approximately. This could represent the duration of one half of a performance. If the initial temperature in the auditorium was warmer than the desired temperature, then if the ventilation vents were open for the whole of the first-half performance, transient ventilation described in § 3 could persist for the whole of the first-half performance. This would lead to the audience being substantially colder than the desired steady temperature until times close to the end of the performance. In order to manage this, the vents could be gradually opened during the performance, so that the temperature of the lower layer fluid remains close to the desired temperature. If the initial temperature in the auditorium were colder than the exterior, as may occur during the day in summer, then during the first-half performance, the air flow may follow the descending ventilation regime of § 4. In this case, the audience could continue to breath air from the lower layer for a considerable time, and would not receive substantial amounts of fresh external air until the overturn mixing event occurred (figure 10*a*). During this time, CO_2 levels would build up, perhaps leading to unsatisfactory conditions even though the temperature remains cooler than the exterior. In order to provide fresh air to the audience, the space might require over-ventilation during the early part of the performance, in order to accelerate the mixing event, and the onset of upward displacement ventilation. We plan to study these applications in more detail elsewhere.

Appendix

In this Appendix we discuss the development of the mixed zone above the interface due to the motion of the convective plumes at the interface. With heat flux Q, the typical convection speed, v, a distance h above the heated boundary scales as

$$v \sim (\alpha g Q h / \rho C_p)^{1/3} \tag{A 1}$$

where α is the thermal expansion coefficient, g the acceleration due to gravity, ρ the density and C_p the specific heat. Given the heat flux Q per unit area, supplied from the lower boundary, we therefore expect the temperature elevation of such convective plumes to scale as

$$\Delta T \sim \frac{Q}{\rho C_p v} \tag{A 2}$$

relative to the lower layer fluid, T_l. When these plumes reach the interface with the upper layer fluid, they are carried by their momentum some distance into the upper layer. If the upper layer is of higher temperature than the plumes, $T_u - T_l > \Delta T$, then

the plumes may rise a distance which scales as

$$h_p \sim \frac{v^2}{g\alpha\Delta T} \tag{A 3}$$

and then fall back. This zone of intermediate temperature supplies a conductive flux of heat into the lower layer which may dominate the effects of entrainment at early times, but as the mixed layer deepens, such conductive fluxes also decrease. The rate of deepening of the mixed layer can be estimated, in a simple way, by considering the effective mixing diffusivity which scales with v and h_p, $\kappa_e \sim vh_p$. This is typically much larger than κ, the molecular diffusivity.

In the present problem, if the initial temperature is significantly greater than the original temperature, then the rate of such deepening will be small compared to the rate of ventilation. As an example, we consider typical values appropriate for a large auditorium or Hall of vertical extent 10 m, and with a heat load of order $Q \sim 30\,\mathrm{W\,m^2}$ on the floor. Such auditoria require 3–4 air changes per hour, so that the time scale of interest is 1000—2000 s. The convective velocities at a height of 3–5 m above the floor, in the lower layer, scale as 0.13–0.16 $\mathrm{m\,s^{-1}}$ and the associated temperature anomalies scale as 0.2–0.3 °C. The Péclet number of such convection, $(vh_p/\kappa) \sim 2 \times 10^5$, is large. Therefore with a temperature contrast of 1–3 °C across the interface, we expect reasonably vigorous penetrative convection. Indeed, using the above scalings, we expect that upper layer fluid will be entrained into the lower layer at a rate of about 0.001–0.002 $\mathrm{m\,s^{-1}}$, and that the lower layer plumes may rise up to nearly 0.05 m into the original upper layer. The effective diffusivity vd_p therefore scales as $10^{-3}\,\mathrm{m^2\,s^{-1}}$. Using these scalings, we infer that this could generate a mixed zone of order 1 m deep over a time of 1000 — 2000 s. We deduce that if, during the ventilation of the upper layer, the lower layer remains colder than the upper layer, then the penetrative convection may entrain of order 1 m of the upper layer fluid into the lower layer, and the plume-driven mixing may produce an intermediate mixed zone of order 1 m deep. In buildings of depth 10 m or greater, the effects of such penetrative convection are not negligible, but are dominated by the effects of floor heating and upward ventilation flow. In such cases, equation (A 1) can provide an indication of the impact of the penetrative entrainment on the overall evolution of the system, in accord with our experimental observations (§ 5). In contrast, in buildings of smaller vertical extent, penetrative convection may be much more important in mixing the upper and lower layers, and thereby in producing a more continuously stratified interior.

We also note that if the temperature contrast between layers is small, then, owing to the floor heating, the convective plumes rising to the interface may be hotter than the upper layer. As a result, they may continue mixing into the upper layer, producing an extended mixing zone and ultimately a well-mixed interior.

Guided by these scalings, we restrict application of the simplified model (A1) to buildings in which the ventilation is relatively rapid compared to the time for mixing, so that the interface remains relatively localized. For less well-ventilated buildings, with interior spaces of small vertical extent, or only a small temperature contrast between the original hot layer and the new lower layer, then the effect of the penetrative convection will be more substantial and a more complete model of the turbulent mixing zone would be required. Owing to the challenge of describing such turbulent mixing, this will form the subject of further study. The present model does however allow us to examine the competition between the ventilation and the

heating, with our model (A1) providing a simple indication of the effects of any weak penetrative convection on this balance.

REFERENCES

Caulfield, C. P. & Woods, A. W. 2002 The mixing in a room by a localized finite-mass-flux source of buoyancy. *J. Fluid Mech.* **471**, 33–50.

Cooper, P. & Linden, P. F. 1996 Natural ventilation of an enclosure containing two buoyancy sources. *J. Fluid Mech.* **311**, 153–176.

Deardorff, J. W., Willis, G. E. & Lilly, D. K. 1969 Laboratory investigation of non-steady penetrative convection. *J. Fluid Mech.* **35**, 7–31.

Denton, R. A. & Wood, I. R. 1981 Penetrative convection at low Péclet number. *J Fluid Mech.* **111**, 1–21.

Fitzgerald, S. D. & Woods, A. W. 2004 Natural ventilation of a room with vents at multiple levels. *Building and Environ.* **39**, 505–521.

Gladstone, C. & Woods, A. W. 2001 On buoyancy-driven natural ventilation of a room with a heated floor. *J. Fluid Mech.* **441**, 293–314.

Haywood, R. W. 1972 *Thermodynamic Tables in SI (metric) Units.* Cambridge University Press.

Kaye, N. B. & Hunt, G. R. 2004 Time-dependent flows in an emptying filling box. *J. Fluid Mech.* **520**, 135–156.

Linden, P. F. 1999 The fluid mechanics of natural ventilation. *Annu. Rev. Fluid Mech.* **31**, 201–238.

Linden, P. F. & Cooper, P. 1996 Multiple sources of buoyancy in a naturally ventilated enclosure. *J. Fluid Mech.* **311**, 177–192.

Linden, P. F., Lane-Serff, G. F. & Smeed, D. A. 1990 Emptying filling boxes: the fluid mechanics of natural ventilation. *J. Fluid Mech.* **212**, 309–335.

Lister, J. A. 1995 On penetrative convection at low Péclet number. *J. Fluid Mech.* **292**, 229–248.

Zilitinkevich, S. S. 1991 *Turbulent Penetrative Convection.* Avebury.